

Study of the online event filtering algorithm for BESIII*

FU Cheng-Dong(傅成栋)^{1,2;1)} ZOU Jia-Heng(邹佳恒)^{3;2)} MO Xiao-Hu(莫晓虎)^{2;3)} HE Kang-Lin(何康林)^{2;4)}
 BIAN Jian-Ming(边渐鸣)^{2,4} CAO Guo-Fu(曹国富)^{2,4} CAO Xue-Xiang(曹学香)^{2,4} CHEN Shen-Jian(陈申见)⁵⁾
 DENG Zi-Yan(邓子艳)² GAO Yuan-Ning(高原宁)¹ HE Miao(何苗)^{2,4} HUA Chun-Fei(花春飞)⁶⁾
 HUANG Bin(黄彬)^{2,4} HUANG Xing-Tao(黄性涛)³ JI Xiao-Bin(季晓斌)² LI Fei(李飞)²⁾
 LI Hai-Bo(李海波)² LI Wei-Dong(李卫东)² LIANG Yu-Tie(梁羽铁)⁷ LIU Chun-Xiu(刘春秀)²⁾
 LIU Huai-Min(刘怀民)² LIU Qiu-Guang(刘秋光)^{2,4} LIU Suo(刘锁)⁸ LIU Ying-Jie(刘英杰)²⁾
 MA Qiu-Mei(马秋梅)² MA Xiang(马想)^{2,4} MAO Ya-Jun(冒亚军)⁷ MAO Ze-Pu(毛泽普)²⁾
 PAN Ming-Hua(潘明华)⁹ PANG Cai-Ying(庞彩莹)⁹ PING Rong-Gang(平荣刚)² QIN Gang(秦纲)^{2,4)}
 QIN Ya-Hong(秦亚红)⁶ QIU Jin-Fa(邱进发)² SUN Sheng-Sen(孙胜森)² SUN Yong-Zhao(孙永昭)^{2,4)}
 WANG Ji-Ke(王纪科)^{2,4} WANG Liang-Liang(王亮亮)^{2,4} WEN Shuo-Pin(文硕频)²⁾
 WU Ling-Hui(伍灵慧)^{2,4} XIE Yu-Guang(谢宇广)^{2,4} XU Min(徐敏)¹⁰ YAN Liang(严亮)^{2,4)}
 YOU Zheng-Yun(尤郑昫)⁷ YU Guo-Wei(俞国威)² YUAN Chang-Zheng(苑长征)² YUAN Ye(袁野)²⁾
 ZHANG Bing-Yun(张炳云)² ZHANG Chang-Chun(张长春)² ZHANG Jian-Yong(张建勇)^{2,11)}
 ZHANG Xue-Yao(张学尧)³ ZHANG Yao(张瑶)³ ZHENG Yang-Heng(郑阳恒)⁴⁾
 ZHU Ke-Jun(朱科军)² ZHU Yong-Sheng(朱永生)² ZHU Zhi-Li(朱志丽)⁹⁾

1 (Tsinghua University, Beijing 100084, China)

2 (Institute of High Energy Physics, CAS, Beijing 100049, China)

3 (Shandong University, Jinan 250100, China)

4 (Graduate University of Chinese Academy of Sciences, Beijing 100049, China)

5 (Nanjing University, Nanjing 210093, China)

6 (Zhengzhou University, Zhengzhou 450001, China)

7 (Peking University, Beijing 100871, China)

8 (Liaoning University, Shenyang 110036, China)

9 (Guangxi Normal University, Guilin 541004, China)

10 (Department of Modern Physics, University of Science and Technology of China, Hefei 230026, China)

11 (CCAST(World Laboratory), Beijing 100080, China)

Abstract The results of a study of event tagging strategies for elementary physics processes in the τ -charm region are presented. The algorithm for online event filtering is optimized by adopting the information provided by different sub-detectors according to their strengths and capacities. The algorithm is tested with various generated physics and background events. The results indicate that the algorithm satisfies the requirements of BESIII physics analysis and its DAQ system.

Key words trigger rate, event tagging and filtering, characteristic topology of various event

PACS 01.50.Pa, 07.05.Kf, 87.10.Rt

Received 25 July 2007, Revised 23 November 2007

* Supported by CAS Knowledge Innovation Project(U-602, U-34), National Natural Science Foundation of China (10491300, 10491303, 10605030) and 100 Talents Program of CAS (U-25 and U-54)

1) E-mail: fucd@ihep.ac.cn

2) E-mail: zoujh@ihep.ac.cn

3) E-mail: moxh@ihep.ac.cn

4) E-mail: hekl@ihep.ac.cn

1 Introduction

The τ -charm energy region is uniquely situated at the boundary between the perturbative and non-perturbative regimes of quantum chromodynamics (QCD) and, therefore, provides a bonanza of opportunities for research in high energy physics. From 1989 to 2004, the Beijing Electron-Positron Collider (BEPC) and Beijing Spectrometer (BES) have operated successfully. A great number of interesting and exciting of physics results were produced, covering the area of light hadron spectroscopy, properties of the charmonium spectrum, charm meson decay properties, tests of QCD, τ physics, rare decays, glueball searches and the observation of candidates for multi-quark states, and so on^[1].

To meet the competition from other high luminosity accelerators, e.g., CESR/CLEO-c and B factories, both BEPC and BES are being upgraded into BEPC II and BESIII^[2]. The design peak luminosity for BEPC II is $10^{33} \text{ cm}^{-2} \cdot \text{s}^{-1}$ optimized at 1.89 GeV, which will make it the highest luminosity accelerator in τ -charm region ever built^[3]. In addition to e^+e^- collisions, a lot of backgrounds due to beam-gas, beam-lost, cosmic ray, synchrotron radiation and electronics noise are expected to be present. To selectively acquire physics events efficiently, a multi-level data filtering technique will be applied in BESIII. The first level filtering is a fast hardware trigger system, which reduces the event rate from ~ 125 MHz to about 4000 Hz at the J/ψ peak of which half will be due to backgrounds. The second filtering is a software trigger, that aims to suppress background rates by about half. To this end, a detailed study of the algorithm of online event filtering was performed; results of this study are presented in this paper.

2 Physics processes and cross sections in τ -charm energy region

An introduction to the elementary physics processes of τ -charm region can be found in Refs. [3–5]. In this section, the descriptions of the lowest order (α^2) cross sections are recapitulated.

The differential cross section for Bhabha scattering ($e^+e^- \rightarrow e^+e^-$) is expressed as follows

$$\frac{d\sigma}{d\Omega} = \frac{\alpha^2}{4s} \left(\frac{3 + \cos^2\theta}{1 - \cos\theta} \right)^2,$$

where s is the square of center-of-mass (c.m.) energy, α the fine structure constant of electromagnetic interaction, θ the relative angle between the incoming and outgoing electrons. The angular distribution possesses a sharp peak at small angles ($\theta \rightarrow 0$ or π)

due to the spacelike Feymann diagram.

For μ -pair production ($e^+e^- \rightarrow \mu^+\mu^-$), the differential cross section reads

$$\frac{d\sigma}{d\Omega} = \frac{\alpha^2}{4s} (1 + \cos^2\theta).$$

The differential cross section for diphoton annihilation ($e^+e^- \rightarrow \gamma\gamma$) is given by

$$\frac{d\sigma}{d\Omega} = \frac{\alpha^2}{s} \left(\frac{1 + \cos^2\theta}{1 - \cos^2\theta} \right).$$

The angular distribution is strongly peaked towards forward and backward angles.

Taking into account radiative corrections to order α^3 , the cross sections are enhanced around 30%, 15%, and 12% for Bhabha, μ -pair, and diphoton processes, respectively.

Above the $\tau^+\tau^-$ mass threshold, the differential cross section for τ -pair production ($e^+e^- \rightarrow \tau^+\tau^-$) calculated to be as follows

$$\frac{d\sigma}{d\Omega} = \frac{\alpha^2}{4s} \beta [(2 - \beta^2) + \beta \cos^2\theta],$$

where $\beta = \sqrt{1 - \frac{4m_\tau^2}{s}}$, the velocity of the τ particle. The high order corrections for the cross section in the vicinity of the $\tau^+\tau^-$ mass threshold became available recently^[6–9] and the accuracy is now claimed to be at the level of 0.1%.

The cross section for two-photon process ($e^+e^- \rightarrow e^+e^-\gamma^*\gamma^*$), which is concerned with the cross section of $\gamma^*\gamma^* \rightarrow X$, can be found in Ref. [10]. The kinematics of this process favor the emission of particles along beam direction and the effective cross section within the acceptance of detector is rather small. By virtue of BES II experience, the effect of this process on hadronic events is weak^[11] or even negligible^[12, 13]. In this work, no special identification is made for this type of events partly due to comparatively small effect and partly due to the lack of a perfect generator. The detail study for the effect of the two-photon process to the event filtering will be implemented in the near future.

The total cross section of non-resonance hadron ($e^+e^- \rightarrow \gamma^* \rightarrow \text{hadrons}$) is often expressed in terms of the R -value as

$$\sigma_{e^+e^- \rightarrow \text{hadrons}} = \sigma_{e^+e^- \rightarrow \mu^+\mu^-} \cdot R.$$

Here

$$\sigma_{e^+e^- \rightarrow \mu^+\mu^-}^0 = \frac{4\pi\alpha^2}{s} \approx \frac{86.8[\text{nb}]}{s[\text{GeV}^2]},$$

is the integrated lowest-order cross section for dimuon production. The R -value can be obtained from a perturbative QCD calculation^[14].

The 1^{--} resonance peaks ($e^+e^- \rightarrow \mathcal{R}$) near charm threshold are especially important for physics analyses, since almost all of BESIII data are to be taken

within these regions. The Born-order cross section for a resonance $\mathcal{R} \rightarrow e^+e^-$ can be described by the well-known Breit-Wigner formula

$$\sigma(s) = \frac{12\pi\Gamma_e\Gamma}{(s - M^2) + M^2\Gamma^2},$$

where Γ_e denotes the partial decay width of $\mathcal{R} \rightarrow e^+e^-$; Γ the total decay width of \mathcal{R} ; M the corresponding mass; and \sqrt{s} the c.m. energy.

The cross section for e^+e^- collisions incorporating radiative corrections to the Born order term is provided in Refs. [15, 16] For narrow resonances like the J/ψ and ψ' , the effects of beam energy spread have to be taken into account^[11, 17].

The corresponding integrated cross sections for the above-listed physics processes are calculated as shown in Fig. 1. For Bhabha, μ -pair, and diphoton processes, a detection region corresponding to $|\cos\theta| \leq 0.93$ is utilized which corresponds to the maximum geometry acceptance of BESIII. For resonances, the parameters used are taken from Ref. [18]. Here the acceptances for hadronic final states or those from resonance decays are assumed to be 100 percent, since most of these types of events have comparatively large multiplicities.

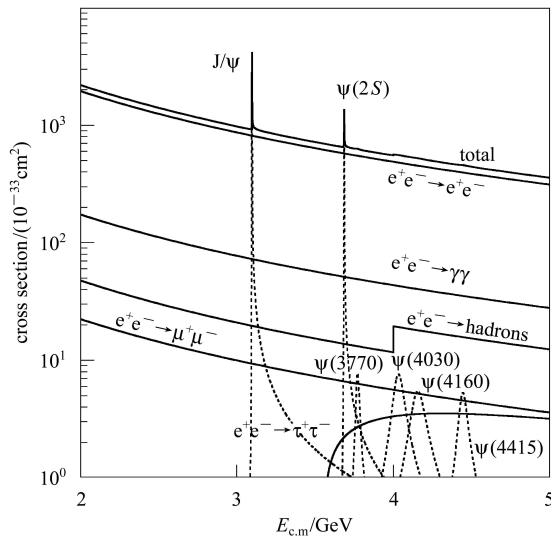


Fig. 1. Cross sections of various physics processes in τ -charm energy region. All resonances are denoted by dashed lines while others solid lines.

At BESIII, the largest cross section is achieved at the J/ψ peak, which is as high as ~ 3200 nb; The second largest cross section reached at the ψ' peak, where it is about 700 nb. These can be seen clearly in Fig. 1.

With the known total cross section σ_t (viz. the summation of various aforementioned processes), the event rate ν can be obtained from the formula

$$\nu \equiv \frac{N}{t} = \sigma_t \cdot L,$$

where N and t are the measured number of events and the corresponding time interval, respectively. For BESIII, the design luminosity is $L_0 = 10^{33} \text{ cm}^{-2} \cdot \text{s}^{-1}$ or $1 \text{ nb}^{-1} \cdot \text{s}^{-1}$ at $E_b = 1.89 \text{ GeV}$. Herein with the L_0 luminosity, if the total cross section is presented in units of nb, the numerical value of ν coincides with that of σ_t , thus Fig. 1 could also be regarded as the variation of event rate against energy, with Hz as the unit of the ordinate.

During experimental data taking, the samples are actually a mixture of physics and background events, and the online filtering system has to play the important roles of event classification and background suppression.

3 The Event filtering system

3.1 The BESIII detector

The BESIII detector is described in detail elsewhere^[2, 19]; here only a short recapitulation of the relevant features is provided. The BESIII detector consists of a beryllium beam pipe, a helium-based small-celled drift chamber (MDC), Time-Of-Flight (TOF) counters for particle identification, a CsI(Tl) crystal calorimeter (EMC), a superconducting solenoidal magnet with the field of 1 Tesla, and a muon identifier comprised of Resistive Plate Counters (RPC) interleaved with the magnet yoke plates (MUC).

The hardware trigger system (Level 1 trigger) uses a pipelined technique based on FPGAs in order to sample events swiftly; information from all sub-detector is employed. The maximum trigger rate at the J/ψ resonance will be about 4000 Hz with about 2000 Hz of that rate due to physics events of interest. The entire data acquisition system (DAQ) has been tested successfully with ~ 6000 Hz trigger rates. The preliminary version of the BES Offline Software System (BOSS)^[20] is complete and the corresponding detector simulation^[21] is based on the Geant4^[22] package.

To suppress background events more efficiently and store physics events economically, a software trigger system (Level 2 trigger) is designed to run on the DAQ computer farms. It will provide two major online functionalities: event filtering and event classification.

3.2 The framework of the event filtering system

The event filtering software (EVF) is part of the DAQ system. When a physics or background event passes the Level 1 trigger, the DAQ system will collect all information from the sub-detectors and send

the event buffer to the Level 2 trigger system. Most of background events will be rejected by the event filter software, and $\sim 100\%$ physics events will be kept. To keep the DAQ system running smoothly, the average latency of the EVF is designed to be less than 5 ms. Both fast processors and a fast algorithm are required.

The framework of the event filtering system^[23] is developed based on a step-by-step technique from Gaudi^[24] and the software trigger system of the ATLAS^[25] experiment. It provides the controller for the algorithm configuration which is composed of global and local algorithms. The former defines the running conditions while the latter defines program components and variables to be used for each sub-detector.

Sometimes, fast reconstruction algorithms are needed to improve the capacity of event identification. The applied algorithms include a fast track reconstruction that finds the charged tracks in the MDC^[26], and a fast cluster finding algorithm that searches for clusters in the EMC^[27]. For an event, the CPU time of the fast algorithms are estimated to be less than several milliseconds.

3.3 Event generation

Currently, experimental data from the BESIII detector are not available, so the algorithm for the event filtering software is developed based on Monte Carlo data on the offline platform.

A sample of Bhabha scattering events is generated using Bhlumi^[28] which includes up to α^4 order radiation corrections. Diphoton events are generated with radgg^[29] with an accuracy that is around α^3 . The μ -pair, τ -pair and hadron events are generated by KKMC, which is the generally utilized simulation system for inclusive processes^[30, 31]. The prominent feature of KKMC is the incorporation of initial-final state interference in a coherent exclusive exponentiation scheme that maintains full control over the spin

polarization for all fermions. Such generator, which is applicable to the difficult case of narrow resonance, can produce Monte Carlo simulations with a precision of better than 1% for c.m. energies between τ threshold and 1 TeV.

The decay of particles produced by the physics generators are handled by EvtGen^[32], in which decay amplitudes, rather than probabilities, are used for each node in the decay tree to simulate the entire decay chain, including all angular correlations.

The background events are produced with special generators. The beam-gas sample is generated through interaction between electron/positron and beam-gas^[33]; the cosmic ray sample is generated according to the energy and angular distribution that are described in Ref. [18].

4 Algorithm of event selection

To get an accurate classification and fast identification for various events, usually many experimental quantities have to be employed, exploiting the particular features of each sub-detector, the characteristic topology of the event type, and so on. Both the information and the sequence for each sub-detector have been scrutinized to acquire an optimized algorithm. Fig. 2 shows the flow chart of the online event filtering algorithm, which displays the optimized sequence for using various pieces of information. The advantage of such an algorithm will be seen more clearly in Sec. 5.2.

The number of hits in each sub-detector may provide a fast criterion for rejecting events caused by an unusual detector response. Monte Carlo study indicates that the total number of hits (N_{hits}) in the MDC for normal physics event is usually less than 1000. A reasonable cut (e.g. < 1000) on the number of hits in the MDC can reject this type of background event, which might cause the reconstruction program to hang up.

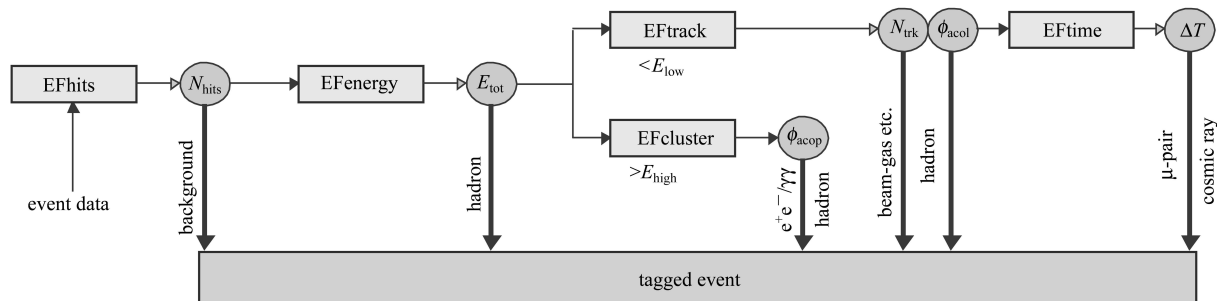


Fig. 2. The flow chart of online event filtering algorithm. Here rectangles indicate the sub-algorithm while the quantities in circles are corresponding variables utilized by the sub-algorithm. For example, EFenergy is a sub-algorithm which realizes the event selection relevant to of E_{tot} . As to other sub-algorithms and corresponding variables, the expound can be found in the text.

4.1 The characteristic topology of various events

Events that pass the criterion on the number of hits in each sub-detector are subjected to a series of algorithms. Depicted in this section are the important characteristic topology features of various physics and background events.

4.1.1 Total energy deposit in EMC

The total energy deposited in the EMC (E_{tot}) is a powerful variable for event classification. E_{tot} is determined from $E_{\text{tot}} = \sum_i^N c_i \cdot \text{ADC}_i$, where ADC_i and c_i represent the raw ADC value and the corresponding uniformity constant for the i -th crystal, N is the number of crystals. The normalized E_{tot} is a flexible variable in different energy point. Here and after, the symbol with tilde on the head indicates that the variable is normalized by c.m. energy. For example, $\tilde{E}_{\text{tot}} = E_{\text{tot}}/\sqrt{s}$.

Each type of events has its distinctive behavior in the EMC. As shown in Fig. 3, most of hadron events lie at the middle of the distribution; e^+e^- and $\gamma\gamma$ events are crowd at the region with larger energy deposit; and the $\mu^+\mu^-$, cosmic ray, beam-gas, and small fraction of hadron events are located at the low energy region.

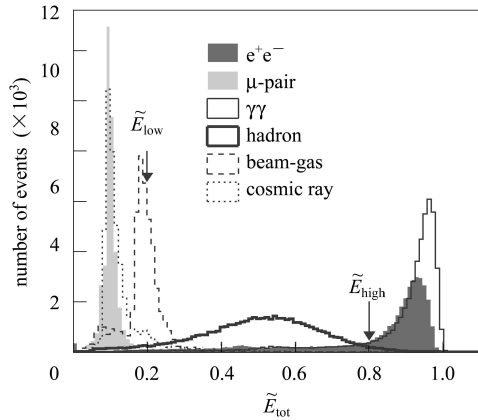


Fig. 3. Total energy deposit in EMC for various types of events, which is normalized to c.m. energy \sqrt{s} .

Two values \tilde{E}_{low} and \tilde{E}_{high} , called respectively low and high threshold of \tilde{E}_{tot} , are used to classify the events as follows: the events with $\tilde{E}_{\text{tot}} > \tilde{E}_{\text{low}}$ and $\tilde{E}_{\text{tot}} < \tilde{E}_{\text{high}}$ are regarded as hadron events, which also include most of τ -pair events; the events with $\tilde{E}_{\text{tot}} > \tilde{E}_{\text{high}}$ can be e^+e^- or $\gamma\gamma$ events which are applied in the luminosity measurements; and the events with $\tilde{E}_{\text{tot}} < \tilde{E}_{\text{low}}$ need further processing to distinguish the physics events from the backgrounds.

4.1.2 Acoplanarity

Bhabha and $\gamma\gamma$ events are needed for online luminosity calculation. They can not be identified merely

by using the information of total energy deposit in the EMC. Since the charged particle is to be bent under the magnetic field while the neutral one is not, events with $\tilde{E}_{\text{tot}} > \tilde{E}_{\text{high}}$ are subjected to a fast algorithm to reconstruct the position of each shower in the EMC.

The acoplanarity angle of two most energetic showers is defined by

$$\cos \phi_{\text{acop}} \equiv -(\cos \varphi_1 \cos \varphi_2 + \sin \varphi_1 \sin \varphi_2)$$

where $\varphi_i (i = 1, 2)$ is the azimuthal angle of each reconstructed shower. ϕ_{acop} can be used to separate e^+e^- from $\gamma\gamma$ events. As shown in Fig. 4, the ϕ_{acop} value for hadron event spreads rather board, ranging from 0° to 180° ; e^+e^- event is required to satisfy $\phi_{\text{acop}} \subset (\phi_2, \phi_3)$, where ϕ_2 and ϕ_3 are the certain cut values; for $\gamma\gamma$ event, the ϕ_{acop} value peaks sharply around zero, therefore the requirement of $\phi_{\text{acop}} < \phi_1$ is applied for $\gamma\gamma$ identification.

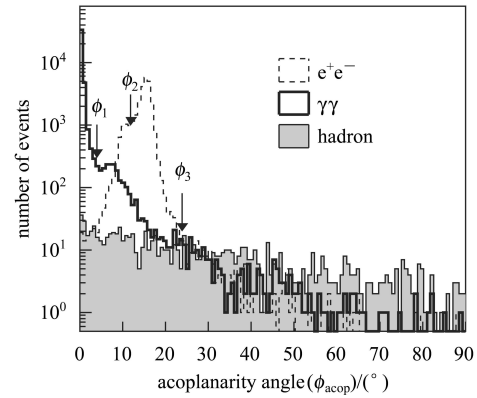


Fig. 4. The distribution of ϕ_{acop} for $\gamma\gamma$, e^+e^- , and hadron events.

4.1.3 Charged track multiplicity and the acollinearity angle

Events with $\tilde{E}_{\text{tot}} < \tilde{E}_{\text{low}}$ are further processed by the fast MDC reconstruction program. Here the powerful variable is the number of charged tracks in the MDC (N_{trk}). As shown in Fig. 5(a), the cosmic ray and beam-gas events have naught reconstructed tracks generally, but only around 10% of hadron events have no reconstructed tracks. Only $\sim 5\%$ of hadron events with low EMC energy, so about 0.5% of hadron events will be discarded by the requirement of at least one reconstructed charged tracks for accepted events. These lost hadron events can hardly be applied in the physics analysis even they are fully reconstructed by the normal offline process.

Most of μ -pair and cosmic ray events are generally reconstructed as two charged tracks in the MDC, which satisfy back-to-back requirement. The acollinearity angle of these two tracks

$$\cos \phi_{\text{acol}} \equiv -(\cos \varphi_1 \cos \varphi_2 \sin \vartheta_1 \sin \vartheta_2 + \sin \varphi_1 \sin \varphi_2 \sin \vartheta_1 \sin \vartheta_2 + \cos \vartheta_1 \cos \vartheta_2)$$

where ϑ_i and $\varphi_i (i=1,2)$ are the reconstructed polar and azimuthal angles of two charged tracks. Similar to the distribution of acoplanarity, the acollinearity tends to zero for μ -pair and cosmic ray events but distributes fairly flat for hadron events.

The number of hits in the MUC (N_{muc}) is checked to ensure it is a μ -contained final state as shown in Fig. 5(b). After that, as candidates, they will be sent to an algorithm which uses the TOF information to identify the μ -pair and cosmic ray event.

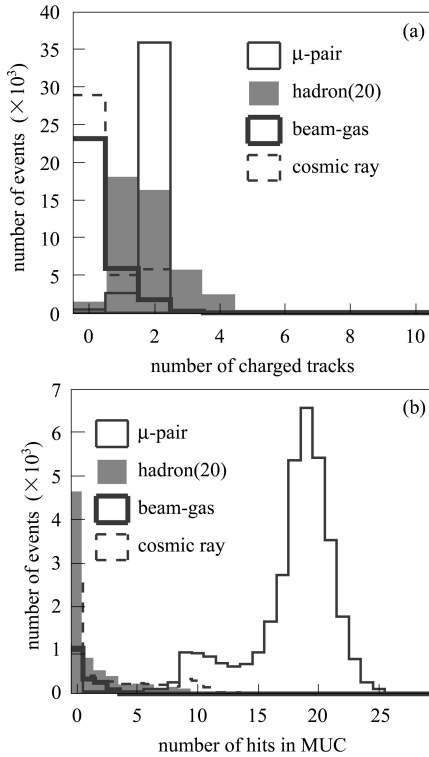


Fig. 5. (a) Number of charged track by the fast MDC reconstruction program; (b) Number of hits in the MUC for back-to-back events. The hadron sample is scaled by a factor of 20 in (a) and 10 in (b).

4.1.4 The difference of time-of-flight

The cosmic ray track traverses from the outer most detector to the beam pipe, then from the beam pipe to the outer most detector. For a collided μ -pair event, both two tracks traverse from the beam pipe to the outer most detector. The difference of time-of-flight in the corresponding upside and downside TOF counters can be used to separate μ -pair from cosmic ray event.

Figure 6(a) shows the distribution of simulated $\Delta T = T_1 - T_2$ for μ -pair and cosmic ray events, where T_1 and T_2 are the measured time-of-flight in the corresponding upside and downside TOF counters. The μ -pair events peak around zero, but most of the cosmic ray events distribute less than -5 ns since the cosmic ray track always hits the upside TOF counter early.

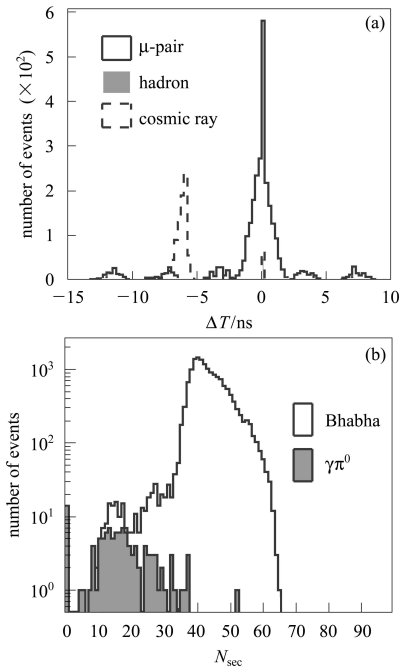


Fig. 6. (a) ΔT distribution for μ -pair and cosmic ray events; (b) the distribution of N_{sec} for Bhabha and $\gamma\pi^0$ events; (b) events are generated as the mixture of Monte Carlo sample and backgrounds.

4.2 Pre-scaling the endcap Bhabha events

At BESIII, Bhabha events are rather abundant for detector calibration and luminosity measurement. Above the charm threshold, the cross section for Bhabha scattering, especially for the small angle scattering, is much higher than that of the interesting physics process. In order to reduce the tape burden, pre-scaling the endcap Bhabha events is in plan.

The Bhabha event is identified solely by utilizing the EMC information, so the endcap Bhabha (EBB) event is confirmed if the two most energetic showers are formed in the endcap detector. The EBB events will be pre-scaled during data taking if necessary.

Some of pure neutral channel hadron events, e.g., $J/\psi \rightarrow \gamma\pi^0$, could be misidentified as the EBB event. To reduce the misidentification rate, the number of hits (N_{sec}) in MDC sector along the direction of EMC showers are carefully checked. As shown in Fig. 6(b), the cut value of N_{sec} around 35 can separate EBB from $J/\psi \rightarrow \gamma\pi^0$ events very efficiently.

4.3 Online luminosity monitoring

The three QED processes $e^+e^- \rightarrow e^+e^-$, $e^+e^- \rightarrow \mu^+\mu^-$, and $e^+e^- \rightarrow \gamma\gamma$, which have salient experimental topology character and accurate theoretical calculated cross section, are conventionally adopted for the luminosity measurement. But at the resonance region, the effects due to leptonic decays of resonance to e^+e^- and/or $\mu^+\mu^-$ must be taken into account. Table 1 shows the e^+e^- , $\mu^+\mu^-$, and $\gamma\gamma$ cross section

ratios of the resonance to the QED process at the J/ψ , ψ' , and ψ'' peaks, respectively. As far as luminosity measurement is concerned, all e^+e^- , $\mu^+\mu^-$, and $\gamma\gamma$ events can be used at the ψ'' peak; both $\gamma\gamma$ and e^+e^- final states can be adopted at the ψ' ; but only $\gamma\gamma$ channel is suitable at the J/ψ .

Table 1. e^+e^- , $\mu^+\mu^-$ and $\gamma\gamma$ cross section ratios of the resonance to the QED process at the J/ψ , ψ' , and ψ'' peaks with $|\cos\theta| \leq 0.93$. The branching ratios in PDG2006 are used in calculation. And the cross section for $\psi'' \rightarrow \mu^+\mu^-$ is taken same as $\psi'' \rightarrow e^+e^-$. The branching ratio of $\psi'' \rightarrow \gamma\gamma$ is referenced by $\psi' \rightarrow \gamma\gamma$.

final state	J/ψ	ψ'	ψ''
e^+e^-	0.21	0.0081	1.3×10^{-7}
$\mu^+\mu^-$	18.2	0.696	$\sim 1.17 \times 10^{-5}$
$\gamma\gamma$	< 0.02	$< 2 \times 10^{-3}$	$< 1.9 \times 10^{-5}$

The integrated luminosity can be calculated as $L = \frac{N}{\epsilon \cdot \sigma}$, where N is the observed number of events for certain final state, ϵ is the selection efficiency (70%–80% for e^+e^- , $\mu^+\mu^-$, and $\gamma\gamma$ at the J/ψ peak), σ is the theoretical cross section. It should be pointed out that the estimated number of background events must be subtracted from the observed events.

Several processes can be used as online luminosity monitoring, especially the endcap Bhabha scattering process is ideal for online luminosity monitoring due to the large cross section and low (physics) background contamination. The results will be compared with the offline measurements by using the events from the large angle Bhabha scattering. In the experimental data taking, we may make reasonable choices among all possible measurements.

5 Performance of the event filtering algorithm

The event filtering algorithm is developed in the offline environment, and will run in both the offline

and online platforms. Since most of the interesting physics topics of BESIII focus on the charmonium states near threshold, various physics samples are generated in offline farm by virtue of their cross sections at the J/ψ , ψ' , and ψ'' peaks. A minimum sets of offline environment with all necessary libraries have been setup at the DAQ farm. Several performance tests have been made on the online computer.

5.1 The filtering efficiencies

The luminosity of BEPCII is optimized at E_b (beam energy)=1.89 GeV, the event filtering efficiencies for various physics processes and background contributions at this energy point are listed in Table 2. The filtering efficiency is defined as $\epsilon_{ij} = N_j/N_i$, where N_j is the number of tagged type j events, N_i is the number of triggered (level 1) type i events, i and j denote the event classification such as e^+e^- , $\mu^+\mu^-$, $\gamma\gamma$, hadron, cosmic ray, beam-gas, and so on. The cross identification is not allowed in the present algorithm, it leads to $\sum_j \epsilon_{ij} = 1$.

All types of events can be classified into two major categories: the physics or background. Here more concerned are the physics efficiency and background suppression rate. As shown in Table 2, the physics efficiencies of the algorithm approximate 100%; about 70% of cosmic ray and 50% of beam-gas backgrounds are suppressed by the filtering algorithm.

Some of decay channels which may have large probability to be lost on the Level 1 trigger^[34] and filtering stage are studied, such as $J/\psi \rightarrow K_L K_S$, $J/\psi \rightarrow \Xi \bar{\Xi}$ and so on. We found that the efficiencies for most of these processes also approximate 100%.

The identification efficiency for endcap Bhabha scattering event is about 71%, while only a few percents of other physics events are misidentified as endcap Bhabha. To reject some of endcap Bhabha events at filtering stage is pretty safe. It is an efficient way to reduce the pressure of huge data record and storage at BESIII, especially for the detector running above the charm threshold.

Table 2. The filtering efficiencies and background suppression rates at $E_b=1.89$ GeV. The numbers are obtained by the following default criteria: $\bar{E}_{low} = 0.2$, $\bar{E}_{high} = 0.8$, $\Delta T = -5$ ns, $\phi_1 = 4^\circ$, $\phi_2 = 10^\circ$, $\phi_3 = 25^\circ$, $\phi_{acol} = 10^\circ$, $N_{sec} = 35$, $N_{trk} = 1$ and $N_{muc} = 5$.

$E_b=1.89$ GeV	physics events					total	background events		
	barrel e^+e^-	endcap e^+e^-	μ -pair	$\gamma\gamma$	hadron		beam gas	cosmic	total
barrel e^+e^-	78.25%	0.04%	1.16%	0.42%	20.13%	100%	0	0	0
endcap e^+e^-	2.82%	71.49%	3.58%	0.21%	21.91%	99.998%	0	0.002%	0.002%
μ -pair	0	0	72.47%	0	26.32%	98.79%	0.97%	0.24%	1.21%
$\gamma\gamma$	0.95%	0.02%	0	80.33%	18.25%	99.55%	0.37%	0.07%	0.45%
hadron	0.49%	0	0.002%	0.27%	99.06%	99.82%	0.04%	0.13%	0.18%
$\tau^+\tau^-$	0	0	0.08%	0	99.81%	99.89%	0.04%	0.07%	0.11%
beam gas	0	0	0	0	50.89%	50.89%	40.86%	8.25%	49.11%
cosmic	0.01%	0	0.10%	0.01%	32.62%	32.75%	1.08%	66.17%	67.25%

5.2 The running time performance

At beginning, the event filtering system is designed to process each event over all sub-algorithms without skipping any sub-algorithm. In this stage, all sub-algorithms are carefully trained and adjusted, moreover bugs are fixed also. However, such a running is really a CPU-time consuming procedure, especially for the hadron and beam gas events. As shown in Fig. 7(a), the averaged CPU-time of this algorithm is about 9 ms which exceeds the requirement allowed by the DAQ system.

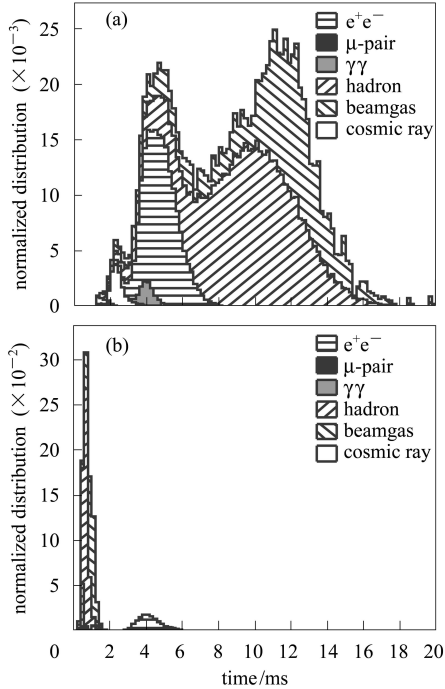


Fig. 7. The running CPU time distributions for various events at the J/ψ peak: (a) Events are required to pass all sub-algorithms; (b) Events are handled by the optimized algorithm.

After trying and testing, the global algorithm is redesigned to allow the well identified event by parts of sub-algorithms to skip other sub-algorithms and jump out from the decision sequencer. Most of hadron events pass the algorithm very quickly. The background candidates will be processed by the complicated algorithms to make sure that it is a “well-diagnosed” background before abandonment. To get an accurate online luminosity, the e^+e^- and $\gamma\gamma$ events subjected to the fast EMC reconstruction algorithm is a little bit slow. As shown in Fig. 7(b), the averaged CPU time for the optimal algorithm is about 1.5 ms which is greatly reduced comparing with previous algorithm. It is obvious that the skipping-jumping function is very effective.

About 20 CPU’s will be fully used by the event filtering algorithm during the data taking. By the design of the whole DAQ system, it seems that more

effective algorithms are allowed to be added into the event filtering system. If the data are taken above the charm threshold at BESIII, more beam-related backgrounds will be expected. The total event rate and filtering time depend on the beam status. Additional DAQ computers may be required in the future if the background rate is too high.

5.3 The performance of selection criteria

The filtering efficiencies are checked in details by varying the selection criteria. In the reasonable variation scopes, no significant changes are observed for the physics events. On the contrary, the beam-related background suppression rate depends strongly on the lower threshold of \tilde{E}_{tot} . As shown in Fig. 8, the beam gas background rate reduces from $\sim 50\%$ to $\sim 20\%$ when the value of \tilde{E}_{low} increases from 0.2 to 0.3. At the same time, the efficiency loss for hadron events is fairly tiny ($< 0.5\%$).

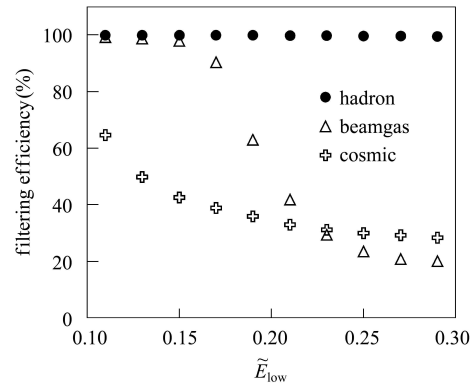


Fig. 8. The variation of filtering efficiencies against \tilde{E}_{low} cut for hadron (denoted by solid circle), cosmic ray (cross) and beam gas (tri-angle) events.

At BESIII, the major backgrounds are the beam-related events (>2000 Hz), the total trigger rate can therefore be adjusted by the value of \tilde{E}_{low} . Anyway, the increasing of \tilde{E}_{low} may introduce extra CPU-time to process more events through the fast MDC reconstruction. To investigate the variations of filtering time, a simple estimation is made by changing the value of \tilde{E}_{low} from 0.2 to 0.3 under different backgrounds rate at the J/ψ peak. The results are summarized in Table 3.

Table 3. The estimation of total event rates and averaged CPU-time per event at the J/ψ peak in different background event rates. Assuming the physics event rates is 2000 Hz and the physics efficiency is 100%.

\tilde{E}_{low}		background rates		
		2000 Hz	4000 Hz	8000 Hz
0.2	total rates	3000 Hz	4000 Hz	6000 Hz
	time/event	1.4 ms	1.4 ms	1.3 ms
0.3	total rates	2400 Hz	2800 Hz	3600 Hz
	time/event	1.7 ms	1.7 ms	1.7 ms

As listed in Table 3, the increase of averaged filtering CPU-time is tolerable since the fast MDC reconstruction is quick enough to process events with low charged multiplicity. The speed of filtering algorithm should not be worried when the value of \tilde{E}_{low} is raised to suppress background rates.

6 Summary

The online event filtering algorithm is developed in the offline environment before merging into the DAQ system. Various physics data are generated, including e^+e^- , $\gamma\gamma$, μ -pair, $\tau^+\tau^-$, $e^+e^- \rightarrow$ hadrons and many interesting physics channels at the J/ψ , ψ' , and ψ'' peaks. The selection criteria are adjusted by comparing the characteristic topology of physics and background events. A fast MDC reconstruction algorithm is adopted for identify backgrounds more reliably. Monte Carlo studies indicate that the present algorithm can satisfy the physics requirements fairly well without detecting significant efficiencies lost for most of physics channels. Anyway the confirmation from experimental test is crucial for the final filtering algorithm.

Comparing with B-factories and LHC experiments in the world, the event rates are quite high at BESIII, especially for the physics event rates. According to the design of the DAQ system, the filtering algorithm must be fast enough to avoid blocking the system. Many optimizations are applied in both the global algorithm and the local algorithms. Lots of test are made in the offline and online platforms. The resulting performances show that the filtering algorithm can satisfy the requirements of the DAQ system.

The filtering system provide several variables to the data monitoring system, such as online luminosity and physics cross section monitoring. The fast EMC reconstruction algorithm is developed to measure the luminosity accurately. The monitoring results have been compared with the offline analyses and they are fairly consistent to each other within the acceptable precisions.

In the future, the event filtering algorithm and selection criteria have to be trained and adjusted with experimental data of BESIII. Further meticulous modifications and improvements in different energy region are necessary by comparing with the normal offline analysis.

References

- 1 BES Collaboration Publications (1992—1999, 2000—2003, 2004—2005), Compiled by BES Collaboration, Internal Reference Books
- 2 Preliminary Design Report: The BESIII Detector, January, 2004
- 3 YUAN Chang-Zheng, ZHANG Bing-Yun, QIN Qing. HEP & NP, 2002, **26**: 1201—1208 (in Chinese)
- 4 Wiik B H, Wolf G. Electron-Positron Interactions. Springer-Verlag, 1979
- 5 Donnachie A, Shaw G. Electromagnetic Interaction of Hadrons (Vol.2). Plenum Press, 1978
- 6 Voloshin M B. Phys. Lett. B, 2003, **556**: 153
- 7 Smith B H, Voloshin M B. Phys. Lett. B, 1994, **324**: 177
- 8 Ruiz-Femenía P, Pich A. Phys. Rev. D, 2001, **64**: 053001
- 9 WANG You-Kai et al. HEP & NP, 2007, **31**: 325
- 10 Brodsky S J, Kinoshita T, Terazawa H. Phys. Rev. D, 1971, **4**: 1532
- 11 BAI J Z et al. (BES Collaboration). Phys. Lett. B, 2002, **550**: 24
- 12 HUANG Guang-Shun. Ph.D. thesis, IHEP of CAS, 1999 (in Chinese)
- 13 HUANG Guang-Shun. Post-Doctor Report, CCAST, 2001
- 14 Surguladze L R, Samuel M A. Phys. Rev. Lett., 1991, **66**: 560; 1991, **66**: 2416
- 15 Kuraev E A, Fadin V S. Sov. J. Nucl. Phys., 1985, **41**: 466; Altarelli G, Martinelli G. CERN, 1986, **86-02**: 47; Nicrosini O, Trentadue L. Phys. Lett. B, 1987, **196**: 551; Berends F A, Burgers G, Neerven W L. Nucl. Phys. B, 1988, **297**: 429; Nucl. Phys. B, 1988, **304**: 921
- 16 Berends F A, Gaemers K J F, Gastmans R. Nucl. Phys. B, 1973, **57**: 381; Berends F A, Komen G J. Nucl. Phys. B, 1976, **63**: 432
- 17 BAI J Z et al. (BES Collaboration). Phys. Lett. B, 1995, **355**: 374
- 18 YAO W M et al. Journal of Physics G, 2006, **33**: 1
- 19 Harris F A et al. (BES Collab.). arXiv:physics/0606059
- 20 LI Wei-Dong, LIU Huai-Min et al. The Offline Software for the BESIII Experiment. Proceeding of CHEP06. Mumbai, India, 2006
- 21 DENG Zi-Yan et al. HEP & NP, 2006, **30**: 371—377 (in Chinese)
- 22 Agostinelli S et al. (Geant4 Collab.). Nucl. Instrum. Methods A, 2003, **506**: 250
- 23 TANG Rui et al. Nuclear Electronics and Detection Technology, 2006, **26**: 95—99 (in Chinese)
- 24 Barrand G et al. Gaudi: The Software Architecture and Framework for Building HEP Data Processing Applications. Comput. Phys. Commun., 2001, **140**: 45
- 25 ATLAS Collaboration. ATLAS: Technical Proposal for a General-Purpose pp Experiment at the Large Hadron Collider at CERN
- 26 ZHANG Xiao-Mei et al. Nuclear Electronics and Detection Technology, 2005, **25**: 638—643 (in Chinese)
- 27 HE Miao et al. Chin. Phys. C (HEP & NP), to be published
- 28 Jadach S et al. Comput. Phys. Commun., 1992, **70**: 305
- 29 Berends F, Kleiss R. Nucl. Phys. B, 1981, **186**: 22
- 30 Jadach S, Ward B F L, Was Z. Comp. Phys. Comm., 2000, **130**: 260
- 31 Jadach S, Ward B F L, Was Z. Phys. Rev. D, 2001, **63**: 113009
- 32 User Handbook. EvtGen: A Monte Carlo Generator for B-Physics, V00-11-07, May 12, 2006
- 33 JIN Da-Peng et al. HEP & NP, 2004, **28**: 1197—1202 (in Chinese)
- 34 SHI Xin, YUAN Chang-Zheng, BAN Yong. HEP & NP, 2004, **28**: 982—985 (in Chinese)